Polymerization-Induced Self-Assembly based on ATRP in Supercritical Carbon Dioxide

Abdullah Alzahrani,[1] Dewen Zhou,[2] Rhiannon P. Kuchel,[3] Per B. Zetterlund,[*,2] and Fawaz Aldabbagh[*,1,4]

[1] *School of Chemistry, National University of Ireland Galway, University Road, Galway, H91 TK33, Ireland*

[2] *Centre for Advanced Macromolecular Design (CAMD), School of Chemical Engineering, The University of New South Wales, Sydney, NSW 2052, Australia*

[3] *Mark Wainwright Analytical Centre, University of New South Wales, Sydney, NSW 2052, Australia.*

[4] *Department of Pharmacy, School of Life Sciences, Pharmacy & Chemistry, Kingston University, Penrhyn Road, Kingston upon Thames, KT1 2EE, UK*

ABSTRACT: Polymerization-induced self-assembly (PISA) based on atom transfer radical polymerization (ATRP) has been performed in supercritical carbon dioxide ($scCO_2$) using a bromo-terminated poly(dimethylsiloxane) (PDMS-Br) species as macroinitiator (solvophilic first block) and poly(benzyl methacrylate) as the solvophobic second block. The polymerizations proceeded to high conversion with good control/livingness. Transmission electron microscopy revealed the formation of the first higher order morphologies in $scCO_2$, namely worms and likely vesicles. Interestingly, highly regular microphase separated multilayered morphology was also observed, which are not observed with PISA carried out in conventional solvents. Overall, the morphologies formed cannot be rationalized based on simple considerations of the relative block lengths and packing parameters, as is typically the case in dispersion PISA in common solvents such as water and water/alcohol. Seemingly, the unique properties of $scCO_2$ lead to different polymer domains.

Over the past decade there has been intense interest in the preparation of non-spherical polymer particles using polymerization-induced self-assembly (PISA).[1-28] PISA is typically implemented as a reversible deactivation radical polymerization (RDRP) in the form of a dispersion polymerization. Most commonly reversible addition-fragmentation chain transfer (RAFT) polymerization is used to extend a solvophilic macroRAFT agent (also acting as steric stabilizer) with a dissolved monomer, which forms the solvophobic polymer core.[1-2, 8-10, 13-16, 18-20, 22, 24, 27-28] PISA can also be implemented as an emulsion polymerization if the monomer is insoluble in the continuous phase.[7, 23] Other RDRP processes have been exploited in connection with PISA, such as atom transfer radical polymerization (ATRP),[3-4, 21] nitroxide-mediated radical polymerization (NMP),[5, 23] organotellurium-mediated living radical polymerization (TERP),[7] and Cu(0)-mediated radical polymerization,[12] as well as recently non-living radical polymerization in the form of addition-fragmentation chain transfer (AFCT) polymerization.[25-26] PISA has been carried out in non-polar solvents,[1-2, 8, 10, 14-17, 20] as well as in more conventional polar media. For instance, higher order non-spherical morphologies, including thermally-sensitive worm-phases, were obtained using RAFT dispersion polymerizations in long chain alkanes via chain extensions of fatty acid-chain containing RAFT agents with benzyl methacrylate (BzMA).[8, 10, 20] RAFT dispersion PISA has also been carried out in ionic liquid, a recyclable green solvent, giving nanoaggregates of multiple morphologies.[11]

Supercritical carbon dioxide ($scCO_2$) is a well-known benign effective replacement for environmentally damaging volatile organic compounds (VOCs).[29-30] CO_2 is cheap and non-flammable with its utility making positive use of a green-house gas. $ScCO_2$ holds considerable merit as a medium for heterogeneous RDRP, in particular precipitation and dispersion polymerizations,[31] given that most vinyl monomers are soluble in $scCO_2$, but the resultant polymer becomes insoluble at a critical degree of polymerization (J_{crit}).[32] Additional advantages of radical polymerization in $scCO_2$ include the easy adjustment of polymer solubility by altering of pressure and monomer loading, and at high conversions venting of the CO_2 leaves a dry polymer powder, which circumvents the requirement for VOC. There are a plethora of reports on dispersion RDRP in $scCO_2$, which are based on two approaches: (*i*) the use of a separate $scCO_2$-soluble steric stabilizer,[33-37] and (*ii*) the use of a $scCO_2$-soluble first block that is subsequently chain extended via RDRP in an approach that is analogous to PISA in conventional media.[38-47] Amphorous fluoropolymers and polysiloxanes are polymers with appreciable solubility in $scCO_2$, and are usually used as macroinitiators for dispersion polymerizations in $scCO_2$. In 1999, Matyjaszewski and DeSimone carried out the first dispersion RDRP in $scCO_2$ by extending bromine-terminated poly(1,1-dihydroperfluorooctyl

methacrylate-Br) with methyl methacrylate (MMA) and 2-(dimethylamino)ethyl methacrylate using ATRP.[38] Okubo and co-workers conducted dispersion ATRP of MMA in $scCO_2$ using bromo-terminated poly(dimethylsiloxane, PDMS-Br), and referred to the $scCO_2$-soluble block as *inistab* (initiator + stabilizer).[39] The *inistab*-concept was consequently used in $scCO_2$ for NMP and iodine transfer dispersion polymerizations using PDMS and fluorinated polymeric alkoxyamines, which were extended with styrene (St) and MMA.[40-43] Howdle and co-workers reported RAFT dispersion polymerizations of MMA and *N*-vinyl pyrrolidine by chain extending fluorinated polymer, PDMS, and polyvinylalkylates.[45-47] However, in all reported dispersion RDRP in $scCO_2$, block copolymer self-assembly has been limited to spherical morphologies.

In the present work, we report the synthesis of a range of higher order morphologies, including worms and vesicles, via PISA in $scCO_2$ implemented with ATRP. There are to date to the best of our knowledge no reports on the dispersion polymerization of BzMA in $scCO_2$, despite its frequent use for PISA in conventional media.[8, 10, 17, 20-21, 25] Chain extensions with BzMA lead to a relatively low glass transition temperature (T_g) in the resultant polymer compared with *e.g.* St and MMA. The lower T_g is associated with increased chain mobility in the core facilitating morphology transition from spheres to worm-like and vesicular morphologies. Herein, PISA is conducted as dispersion ATRP of BzMA in $scCO_2$ using a $scCO_2$ soluble *inistab* species (PDMS-Br) to generate block copolymer particles of various morphologies, including particles with microphase separated multilayered morphology, in one-step at monomer loadings as high as 65 v/v(%). The procedure circumvents the requirement for an aqueous phase or VOCs and conveniently yields polymer particles as a dry powder on venting of CO_2 after polymerization.

Table 1. Summary of molecular weight and conversion data of the specific samples subjected to TEM analysis (dispersion ATRP of BzMA at 80 °C and 30 MPa).

Run[a]	[BzMA] / [PDMS-Br]	BzMA loading v/v(%)	Polymer[b]	$M_{n,th}$ [c]	Conv.[d] (%)[d]	M_n [e]	$Đ$[e]
1	400	35	PDMS-*b*-PBzMA$_{266}$	52550	67	52200	1.33
2	400	35	PDMS-*b*-PBzMA$_{359}$	70900	93	68450	1.34
3	168	35	PDMS-*b*-PBzMA$_{138}$	31400	88	29650	1.25
4	280	35	PDMS-*b*-PBzMA$_{212}$	45900	83	42650	1.25
5	168	50	PDMS-*b*-PBzMA$_{167}$	33200	94	34800	1.33
6	168	65	PDMS-*b*-PBzMA$_{153}$	31700	89	32300	1.30

[a]All polymerization contained [PDMS-Br]/[CuBr]/[HMTETA] = 1:1.5:1.5 and were for 24 h, except Run 2 was 36 h. [b]The degree of polymerization of the BzMA block was obtained by deducting the M_n(GPC) of PDMS-Br (5350 g/mol). The Br-end group is not represented. [c]Calculated according to equation 1 (see SI). [d]Conversion determined by gravimetry. [e]From GPC analysis using linear polystyrene standards.

The appreciable solubility of the monomer BzMA in $scCO_2$ (a requirement for a dispersion polymerization) was visually confirmed using a 100 mL stainless steel reactor with 180° inline sapphire windows, where at 80°C and 30 MPa a transparent solution was observed using 35-65 v/v(%) BzMA loadings. ATRP dispersion polymerizations were subsequently carried out under these conditions in a window-less 25 mL stainless steel reactor at 35 v/v(%) of monomer, initially using [BzMA]:[PDMS-Br]:[CuBr]:[1,1,4,7,10,10-hexmethyltriethylenetetramine; HMTETA] = 400:1:1.5:1.5 (Table 1; Runs 1 and 2; same polymerization receipe taken to different conversions). The *inistab* species PDMS-Br (M_n = 5350 g/mol; $Đ$ = 1.12) was obtained by condensing commercial PDMS-OH with 2-bromoisobutyryl bromide.[39, 48] The polymerizations proceeded to near complete conversion (93%) in 36 h with excellent controlled/living character as indicated by narrow molecular weight distributions (MWDs) with $Đ < 1.35$ and M_n in close agreement with theoretical ($M_{n,th}$) values (Figure 1; note however the GPC data are subject to calibration error using linear polystyrene standards). At the end of the polymerizations, ^{1}H NMR analysis confirmed the complete removal of unreacted monomer by washing the polymer with $scCO_2$ and venting of the CO_2 (containing unreacted monomer). The dry polymer powders (Fig. S1) obtained at the highest conversions (67% after 24 h (Run

1) and 93% after 36 h (Run 2)) were redispersed in pentane, and the particles were subsequently observed by TEM (Fig. 2).

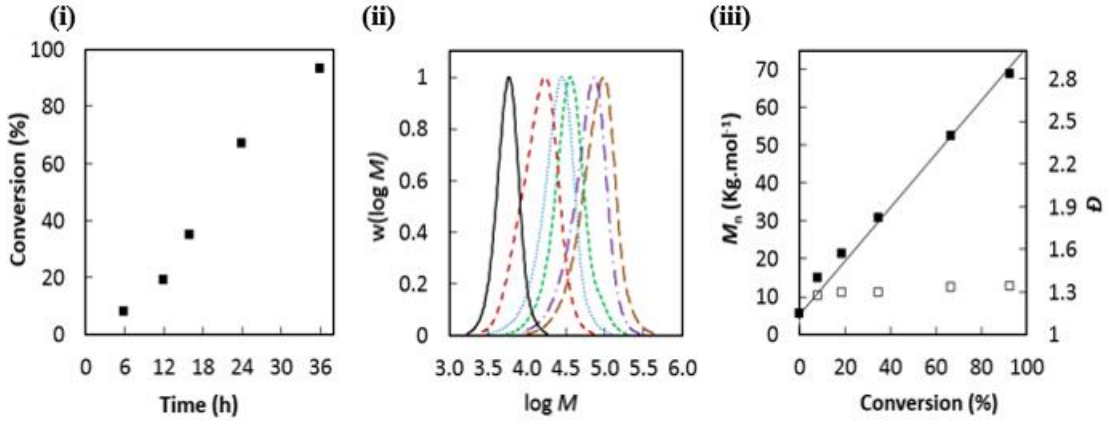

Fig. 1. ATRP dispersion of 35 v/v(%) BzMA in $scCO_2$ at 80 °C and 30 MPa using [BzMA]:[PDMS-Br]:[CuBr]:[HMTETA] = 400:1:1.5:1.5. (i) Conversion vs. time data; (ii) MWDs corresponding to PDMS-Br (black solid line) and polymerizations at conversions of 11 (6 h), 25 (12 h), 40 (16 h), 67 (24 h) and 93% (36 h) (the latter two corresponding to Run 1 and Run 2); (iii) M_n (■) and $Đ$ (□) vs. conversion. $M_{n,th}$ is the continuous line calculated according to equation 1 (see SI).

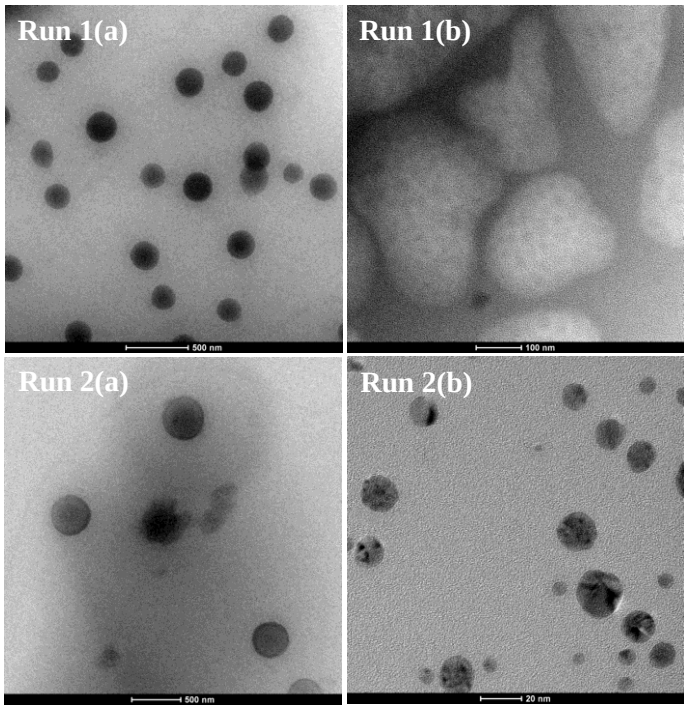

Fig. 2. TEM images of PDMS-*b*-PBzMA particles from Run 1 and Run 2 (Table 1) corresponding to dispersion ATRP at 35 v/v(%) BzMA in $scCO_2$ at 80 °C and 30 MPa. Scale bars are 500 nm (Run 1(a)), 100 nm (Run 1(b)), 500 nm (Run 2(a)) and 20 nm (Run 2(b)).

At 67% conversion (Run 1; DP PBzMA block = 266), the main population comprises near spherical particles with approximate size of 200 nm (Run 1(a)), although non-spherical particles with distinct internal morphology (phase separation) can also be observed (Run 1(b)). At near full conversion of 93%, the phase separation appears more pronounced (Run 2; DP PBzMA block = 359; Fig. 2; Run 2(b)). At this conversion, two distinct solid particle populations were observed of approximate size 300 nm (Fig. 2; Run 2(a)) and 5-30 nm (Fig. 2; Run 2(b)). It seems the particles observed at 67% conversion have increased in size at 93% conversion, and phase separated regions have become smaller spherical particles at higher DP. The effect of the length of the core-forming CO_2-phobic block on the morphology was investigated by reducing the monomer to macroinitiator ratio [BzMA]/[PDMS-Br] while keeping all other parameters constant (Run 3 and Run 4). Narrow MWDs with lower DP values of 138 (Run 3) and 212 (Run 4) for the PBzMA block were obtained after 24 h (Fig. S2). TEM imaging of Run 3 reveals the presence of a population of very small particles (< 10 nm) as well as larger near spherical particles of diameters in the range of 100 – 500 nm that are most likely vesicles, but also wormlike particles. The relatively low T_g of the PBzMA block as well as unreacted BzMA monomer facilitate transition to higher order morphologies. Run 4 resulted in larger irregularly shaped particles of micron-scale dimensions. Interestingly, well-ordered multilayered lamellar phase separated domains on the nanoscale were clearly observable.

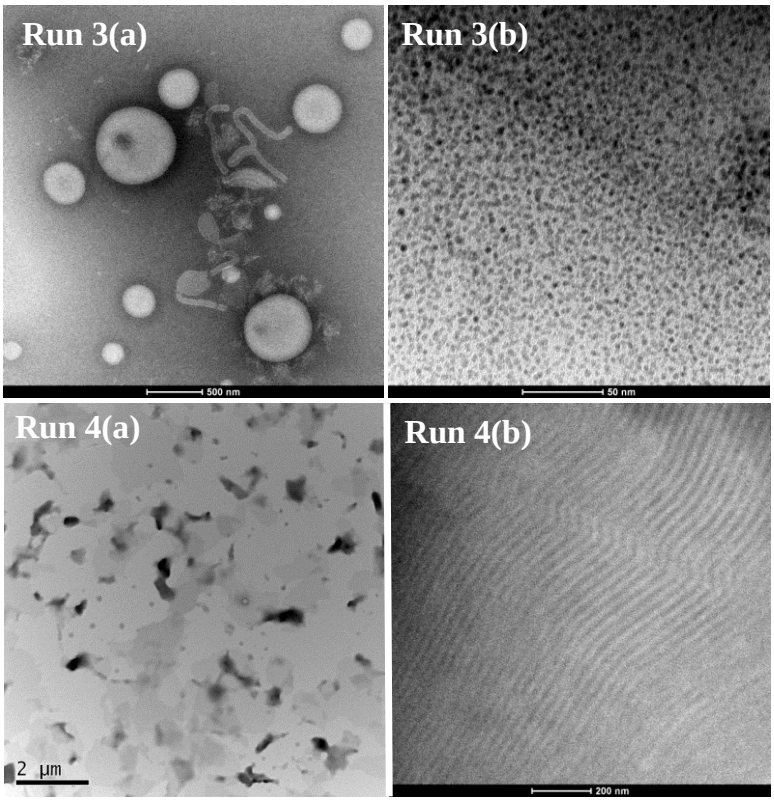

Fig. 3. TEM images of PDMS-*b*-PBzMA particles from Runs 3 and 4 (Table 1) corresponding to dispersion ATRP at 35 v/v(%) BzMA in $scCO_2$ at 80 °C and 30 MPa. Scale bars are 500 nm (Run 3(a)), 50 nm (Run 3(b)), 2 µm (Run 4(a)), and 200 nm (Run 4(b)).

The effect of monomer loading was investigated (35 v/v(%) in Runs 1-4 described so far). The lowest loading of 20 v/v(%) BzMA resulted in low conversion (13%; 24 h) and poor controlled/living character as evidenced by a bimodal MWD (Fig. S3). Poor controlled/living character for nitroxide-mediated radical polymerization (NMP) conducted as precipitation polymerization in $scCO_2$ in previous work has been attributed to the high heterogenity of the system.[49-52] It can be speculated that similar factors are at play in the present ATRP system, with low monomer loadings causing partitioning of reagents (catalyst and ligand) away from the locus of polymerization. The value of J_{crit} is also expected to decrease with decreasing monomer loading, *i.e.* particle formation would occur at lower conversion for 20 v/v(%) BzMA loading,[32] which may cause partitioning effects to become more significant. As the monomer loading was increased beyond 35 v/v(%), excellent controlled/living character was maintained as attested by narrow MWDs ($Đ$ = 1.25-1.33) and high conversions (88-94%) being obtained for 35, 50 and 65 v/v(%) after 24 h (Fig. S3; Runs 3, 5 and 6).

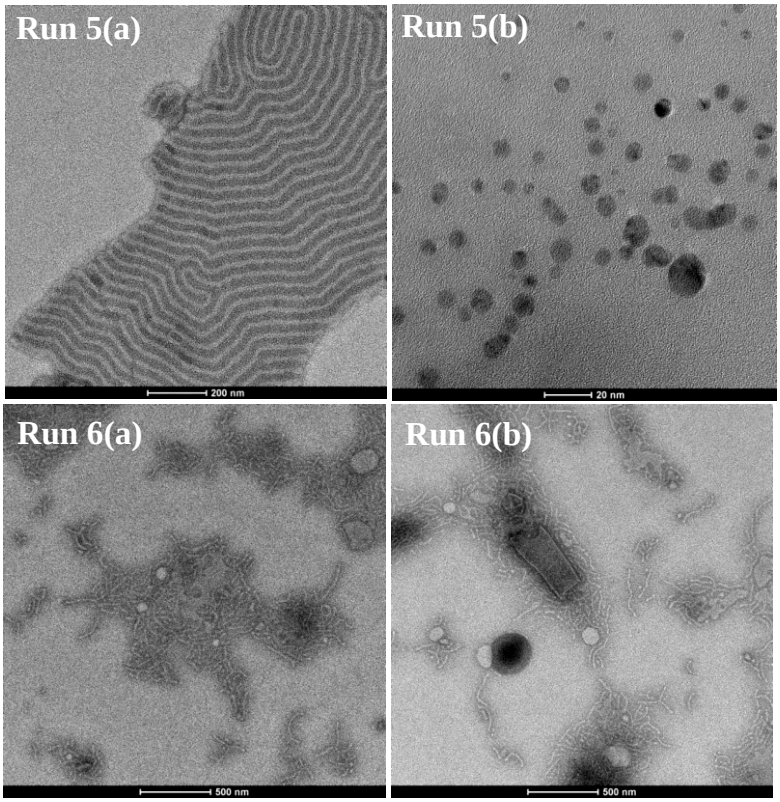

Fig. 4. TEM images of PDMS-*b*-PBzMA particles from Runs 5 and 6 (Table 1) corresponding to dispersion ATRP at 50 (Run 5) and 65 (Run 6) v/v(%) BzMA in $scCO_2$ at 80 °C and 30 MPa. Scale bars are 200 nm (Run 5(a)), 20 nm (Run 5(b)), and 500 nm (Run 6(a) and (b)).

Run 5 resulted in a population of small particles (< 20 nm) with phase separated domains, as well as larger particles featuring very clear multilayered lamellar nanostructured regions. Run 6 yielded mainly worms, but also irregulary shaped particles of approx size 100 – 500 nm.

The particle morphologies obtained via PISA can normally be rationalized based on the packing parameter (*P*), which is given by the relative volume fractions of the stabilizer (PDMS) and core-forming (PBzMA) blocks.[53-54] Normally, an increase in the length of the core forming block would result in a transition towards higher order morphologies, *i.e.* typically from spherical particles to worms and eventually vesicles. The DP of the second block (PBzMA) increases in the order Run 3 (138) < Run 4 (212) < Run 2 (359). These polymerizations were all performed at the same solids content of 35 v/v% and all reached similar high conversion. It is clear that the morphologies depicted in the corresponding TEM images (described above) cannot be rationalized based on the relative block lengths. Interestingly, RAFT dispersion PISA in *n*-heptane generating PDMS-*b*-PBzMA at 70 °C did result in the morphologies evolving from spheres to worms and vesicles as DP of the PBzMA was increased.[17] Run 2, with the highest DP, would be expected to give the highest order morphology, but this polymerization

resulted in two distinct solid particle populations of approximate size 300 nm and 5-30 nm (Fig. 2), whereas Run 3 with the lowest DP of 138 yielded mixed morphologies including worms (Fig. 3). An increase in vol% solids content would normally be expected to drive the morphologies towards higher order morphologies.[19, 55] In the present case, we can compare Run 5 (50 vol% solids) and Run 6 (65 vol% solids), where the DPs of the second blocks were similar. The increase in solids content is accompanied by the appearance of worms (Run 6), compared to two populations of smaller irregularly shaped particles and a population of larger particles observed in Run 5. This trend appears largely consistent with expectation. Comparing Run 5 with Run 3 (35 vol% solids and similar DP as Run 5), the morphologies cannot be rationalzed based on the difference in solids content.

The ”ideal” PISA morphologies of spheres, worms and vesicles comprise structures where the solvophilic block (PDMS in this case) is not buried within the structure. That is, the solvophilic block is typically in direct contact with the continuous phase. As such, multilayered type morphologies as seen for Runs 4 and 5 are typically not observed in PISA. However, it is well established that microphase separation in the solid state (*e.g.* in polymer films) can lead to a number of morphologies similar to those observed for Runs 4 and 5.[56-59] Such microphase separation occurs if the quantity χN is sufficiently high, where χ is the Flory-Huggins segmental interaction parameter and N is the degree of polymerization.[59] It appears that for the present system, at least under the conditions of Runs 4 and 5, the particle formation process leads to structures where the PDMS segment is buried within the structure itself. One can speculate that the presence of $scCO_2$ and its ability to swell the polymer, in particular the PDMS segment, may facilitate the formation of such structures, unlike in ”normal” PISA conducted in conventional solvents such as water and water/alcohol mixtures. Jennings et al.[37] have reported RAFT dispersion polymerization in $scCO_2$ using a PDMS macromonomer as stabilizer (*i.e.* not PISA) in an approach that involved sequential polymerization of two different monomers, thus generating diblock copolymers. These authors found that symmetrical copolymers PMMA-*b*-PSt did not result in the expected morphologies (curved cylindrical domains as opposed to the expected lamellar/multilayered morphology), and this was tentatively attributed to different extents of sorption of CO_2 into the different polymer domains, consistent with how selective sorption can affect the morphology phase diagram.[60] Venting of the CO_2 would subsequently result in these structures being kinetically trapped. It can be speculated that similar factors play a role in our present PISA system, thus leading to unexpected results in terms of the morphology development. Overall, it appears that the morphologies observed in the present dispersion ATRP in $scCO_2$ cannot be rationalized based on the same general considerations as

in conventional PISA. It may be that the unique properties of $scCO_2$ as a solvent exert an influence on the PISA process such that the particle morphologies can no longer be broadly rationalized simply based on the packing parameter.

In summary, we have successfully accomplished the first controlled/living dispersion polymerization in $scCO_2$ to give polymer particles of higher order morphology, including worms and likely vesicles. In addition to morphologies typically observed in dispersion PISA, polymer particles with highly regular multilayered morphology were also observed. Based on the present results, it appears that dispersion PISA in $scCO_2$ is not directly comparable to dispersion PISA in commonly employed media such as water and water/alcohol as well as in hydrophobic solvents, possibly as a consequence of the ability of $scCO_2$ to swell polymer particles / polymer domains. Further optimization is required to fully understand and exploit the potential of $scCO_2$ as a medium for PISA.

ASSOCIATED CONTENT

Supporting Information

The Supporting Information is available free of charge on the ACS Publications website at DOI:

Corresponding Authors

*E-mail: p.zetterlund@unsw.edu.au

*E-mail: f.aldabbagh@kingston.ac.uk

ORCID

Abdullah Alzahrani: 0000-0003-3195-8142

Dewen Zhou

Per B. Zetterlund: 0000-0003-3149-4464

Fawaz Aldabbagh: 0000-0001-8356-5258

Notes

The authors declare no competing financial interest.

ACKNOWLEDGMENTS

We thank the Ministry of Education of the Kingdom of Saudi Arabia for supporting the PhD of AA.

References

1. Houillot, L.; Bui, C.; Save, M.; Charleux, B.; Farcet, C.; Moire, C.; Raust, J. A.; Rodriguez, I., Synthesis of well-defined polyacrylate particle dispersions in organic medium using simultaneous RAFT polymerization and self-assembly of block copolymers. A strong influence of the selected thiocarbonylthio chain transfer agent. *Macromolecules* **2007,** *40* (18), 6500-6509.
2. Houillot, L.; Bui, C.; Farcet, C.; Moire, C.; Raust, J. A.; Pasch, H.; Save, M.; Charleux, B., Dispersion Polymerization of Methyl Acrylate in Nonpolar Solvent Stabilized by Block Copolymers Formed In situ via the RAFT Process. *ACS Appl. Mater. Interfaces* **2010,** *2* (2), 434-442.
3. Sugihara, S.; Sugihara, K.; Armes, S. P.; Ahmad, H.; Lewis, A. L., Synthesis of Biomimetic Poly(2-(methacryloyloxy)ethyl phosphorylcholine) Nanolatexes via Atom Transfer Radical Dispersion Polymerization in Alcohol/Water Mixtures. *Macromolecules* **2010,** *43* (15), 6321-6329.
4. Sugihara, S.; Armes, S. P.; Lewis, A. L., One-Pot Synthesis of Biomimetic Shell Cross-Linked Micelles and Nanocages by ATRP in Alcohol/Water Mixtures. *Angew. Chem. Int. Ed.* **2010,** *49* (20), 3500-3503.
5. Charleux, B.; Delaittre, G.; Rieger, J.; D'Agosto, F., Polymerization-Induced Self-Assembly: From Soluble Macromolecules to Block Copolymer Nano-Objects in One Step. *Macromolecules* **2012,** *45* (17), 6753-6765.
6. Sun, J. T.; Hong, C. Y.; Pan, C. Y., Formation of the block copolymer aggregates via polymerization-induced self-assembly and reorganization. *Soft Matter* **2012,** *8* (30), 7753-7767.
7. Kitayama, Y.; Kishida, K.; Minami, H.; Okubo, M., Preparation of poly(n-butyl acrylate)-b-polystyrene particles by emulsifier-free, organotellurium-mediated living radical emulsion polymerization (emulsion TERP). *J. Polym. Sci.; Part A: Polym. Chem.* **2012,** *50* (10), 1991-1996.
8. Fielding, L. A.; Derry, M. J.; Ladmiral, V.; Rosselgong, J.; Rodrigues, A. M.; Ratcliffe, L. P. D.; Sugihara, S.; Armes, S. P., RAFT dispersion polymerization in non-polar solvents: facile production of block copolymer spheres, worms and vesicles in n-alkanes. *Chemical Science* **2013,** *4* (5), 2081-2087.
9. Zhao, W.; Gody, G.; Dong, S. M.; Zetterlund, P. B.; Perrier, S., Optimization of the RAFT polymerization conditions for the in situ formation of nano-objects via dispersion polymerization in alcoholic medium. *Polym. Chem.* **2014,** *5* (24), 6990-7003.
10. Derry, M. J.; Fielding, L. A.; Armes, S. P., Industrially-relevant polymerization-induced self-assembly formulations in non-polar solvents: RAFT dispersion polymerization of benzyl methacrylate. *Polym. Chem.* **2015,** *6* (16), 3054-3062.
11. Zhang, Q.; Zhu, S. P., Ionic Liquids: Versatile Media for Preparation of Vesicles from Polymerization-Induced Self-Assembly. *ACS Macro Letters* **2015,** *4* (7), 755-758.
12. Kapishon, V.; Whitney, R. A.; Champagne, P.; Cunningham, M. F.; Neufeld, R. J., Polymerization Induced Self-Assembly of Alginate Based Amphiphilic Graft Copolymers Synthesized by Single Electron Transfer Living Radical Polymerization. *Biomacromolecules* **2015,** *16* (7), 2040-2048.
13. Zetterlund, P. B.; Thickett, S. C.; Perrier, S.; Bourgeat-Lami, E.; Lansalot, M., Controlled/Living Radical Polymerization in Dispersed Systems: An Update. *Chem. Rev.* **2015,** *115* (18), 9745-9800.
14. Pei, Y. W.; Noy, J. M.; Roth, P. J.; Lowe, A. B., Soft Matter Nanoparticles with Reactive Coronal Pentafluorophenyl Methacrylate Residues via Non-Polar RAFT Dispersion Polymerization and Polymerization-Induced Self-Assembly. *J. Polym. Sci.; Part A: Polym. Chem.* **2015,** *53* (20), 2326-2335.

15. Pei, Y. W.; Sugita, O. R.; Thurairajah, L.; Lowe, A. B., Synthesis of poly(stearyl methacrylate-b-3-phenylpropyl methacrylate) nanoparticles in n-octane and associated thermoreversible polymorphism. *RSC Advances* **2015,** *5* (23), 17636-17646.
16. Pei, Y.; Thurairajah, L.; Sugita, O. R.; Lowe, A. B., RAFT Dispersion Polymerization in Nonpolar Media: Polymerization of 3-Phenylpropyl Methacrylate in n-Tetradecane with Poly(stearyl methacrylate) Homopolymers as Macro Chain Transfer Agents. *Macromolecules* **2015,** *48* (1), 236-244.
17. Lopez-Oliva, A. P.; Warren, N. J.; Rajkumar, A.; Mykhaylyk, O. O.; Derry, M. J.; Doncom, K. E. B.; Rymaruk, M. J.; Armes, S. P., Polydimethylsiloxane-Based Diblock Copolymer Nano-objects Prepared in Nonpolar Media via RAFT-Mediated Polymerization-Induced Self-Assembly. *Macromolecules* **2015,** *48* (11), 3547-3555.
18. Jennings, J.; He, G.; Howdle, S. M.; Zetterlund, P. B., Block copolymer synthesis by controlled/living radical polymerisation in heterogeneous systems. *Chem. Soc. Rev.* **2016,** *45* (18), 5055-5084.
19. Canning, S. L.; Smith, G. N.; Armes, S. P., A Critical Appraisal of RAFT-Mediated Polymerization-Induced Self Assembly. *Macromolecules* **2016,** *49* (6), 1985-2001.
20. Derry, M. J.; Fielding, L. A.; Armes, S. P., Polymerization-induced self-assembly of block copolymer nanoparticles via RAFT non-aqueous dispersion polymerization. *Prog. Polym. Sci.* **2016,** *52*, 1-18.
21. Wang, G.; Schmitt, M.; Wang, Z. Y.; Lee, B.; Pan, X. C.; Fu, L. Y.; Yan, J. J.; Li, S. P.; Xie, G. J.; Bockstaller, M. R.; Matyjaszewski, K., Polymerization-Induced Self-Assembly (PISA) Using ICAR ATRP at Low Catalyst Concentration. *Macromolecules* **2016,** *49* (22), 8605-8615.
22. Zhou, D.; Dong, S.; Kuchel, R. P.; Perrier, S.; Zetterlund, P. B., Polymerization Induced Self-Assembly: Tuning of Morphology using Ionic Strength and pH. *Polym. Chem.* **2017,** *8*, 3082-3089.
23. Qiao, X. G.; Lamber, O.; Taveau, J. C.; Dugas, P. Y.; Charleux, B.; Lansalot, M.; Bourgeat-Lami, E., Nitroxide-Mediated Polymerization-Induced Self-Assembly of Block Copolymers at the Surface of Silica Particles: Toward New Hybrid Morphologies. *Macromolecules* **2017,** *50* (10), 3797-3807.
24. Yeow, J.; Boyer, C., Photoinitiated Polymerization-Induced Self-Assembly (Photo-PISA): New Insights and Opportunities. *Advanced Science* **2017,** *4* (7).
25. Zhou, D. W.; Kuchel, R. P.; Zetterlund, P. B., A new paradigm in polymerization induced self-assembly (PISA): Exploitation of "non-living" addition-fragmentation chain transfer (AFCT) polymerization. *Polym. Chem.* **2017,** *8* (29), 4177-4181.
26. Lotierzo, A.; Schofield, R. M.; Bon, S. A. F., Toward Sulfur-Free RAFT Polymerization Induced Self-Assembly. *Acs Macro Letters* **2017,** *6* (12), 1438-1443.
27. Tan, J. B.; Li, X. L.; Zeng, R. M.; Liu, D. D.; Xu, Q.; He, J.; Zhang, Y. X.; Dai, X. C.; Yu, L. L.; Zeng, Z. H.; Zhang, L., Expanding the Scope of Polymerization-Induced Self-Assembly: Z-RAFT-Mediated Photoinitiated Dispersion Polymerization. *ACS Macro Letters* **2018,** *7* (2), 255-262.
28. Zaquen, N.; Yeow, J.; Junkers, T.; Boyer, C.; Zetterlund, P. B., Visible Light-Mediated Polymerization-Induced Self-Assembly Using Continuous Flow Reactors. *Macromolecules* **2018,** *51* (14), 5165-5172.
29. Wells, S. L.; DeSimone, J., CO2 technology platform: An important tool for environmental problem solving. *Angew. Chem. Int. Ed.* **2001,** *40* (3), 519-527.
30. Peach, J.; Eastoe, J., Supercritical carbon dioxide: a solvent like no other. *Beilstein J. Org. Chem.* **2014,** *10*, 1878-1895.

31. Zetterlund, P. B.; Aldabbagh, F.; Okubo, M., Controlled/Living Heterogeneous Radical Polymerization in Supercritical Carbon Dioxide. *J. Polym. Sci.; Part A: Polym. Chem.* **2009,** *47* (15), 3711-3728.
32. O'Connor, P.; Zetterlund, P. B.; Aldabbagh, F., Effect of Monomer Loading and Pressure on Particle Formation in Nitroxide-Mediated Precipitation Polymerization in Supercritical Carbon Dioxide. *Macromolecules* **2010,** *43* (2), 914-919.
33. McHale, R.; Aldabbagh, F.; Zetterlund, P. B.; Minami, H.; Okubo, M., Nitroxide-mediated radical dispersion polymerization of styrene in supercritical carbon dioxide using a poly(dimethylsiloxane-b-methyl methacrylate) stabilizer. *Macromolecules* **2006,** *39* (20), 6853-6860.
34. Gregory, A. M.; Thurecht, K. J.; Howdle, S. M., Controlled dispersion polymerization of methyl methacrylate in supercritical carbon dioxide via RAFT. *Macromolecules* **2008,** *41* (4), 1215-1222.
35. Grignard, B.; Jerome, C.; Calberg, C.; Jerome, R.; Wang, W.; Howdle, S. M.; Detrembleur, C., Copper bromide complexed by fluorinated macroligands: towards microspheres by ATRP of vinyl monomers in scCO(2). *Chem. Commun.* **2008,** (3), 314-316.
36. Grignard, B.; Jerome, C.; Calberg, C.; Jerome, R.; Detrembleur, C., Atom transfer radical polymerization of MMA with a macromolecular ligand in a fluorinated solvent and in supercritical carbon dioxide. *Eur. Polym. J.* **2008,** *44* (3), 861-871.
37. Jennings, J.; Beija, M.; Richez, A. P.; Cooper, S. D.; Mignot, P. E.; Thurecht, K. J.; Jack, K. S.; Howdle, S. M., One-Pot Synthesis of Block Copolymers in Supercritical Carbon Dioxide: A Simple Versatile Route to Nanostructured Microparticles. *J. Am. Chem. Soc.* **2012,** *134* (10), 4772-4781.
38. Xia, J. H.; Johnson, T.; Gaynor, S. G.; Matyjaszewski, K.; DeSimone, J., Atom transfer radical polymerization in supercritical carbon dioxide. *Macromolecules* **1999,** *32* (15), 4802-4805.
39. Minami, H.; Kagawa, Y.; Kuwahara, S.; Shigematsu, J.; Fujii, S.; Okubo, M., Dispersion atom transfer radical polymerization of methyl methacrylate with bromo-terminated poly(dimethylsiloxane) in supercritical carbon dioxide. *Designed Monomers and Polymers* **2004,** *7* (6), 553-562.
40. Ryan, J.; Aldabbagh, F.; Zetterlund, P. B.; Okubo, M., First nitroxide-mediated free radical dispersion polymerizations of styrene in supercritical carbon dioxide. *Polymer* **2005,** *46* (23), 9769-9777.
41. McHale, R.; Aldabbagh, F.; Zetterlund, P. B.; Okubo, M., Nitroxide-mediated radical dispersion polymerization of styrene in supercritical carbon dioxide using a poly(dimethyl siloxane-block-styrene) alkoxyamine as initiator and stabilizer. *Macromol. Rapid Commun.* **2006,** *27* (17), 1465-1471.
42. Grignard, B.; Phan, T.; Bertin, D.; Gigmes, D.; Jerome, C.; Detrembleur, C., Dispersion nitroxide mediated polymerization of methyl methacrylate in supercritical carbon dioxide using in situ formed stabilizers. *Polym. Chem.* **2010,** *1* (6), 837-840.
43. Kuroda, T.; Tanaka, A.; Taniyama, T.; Minami, H.; Goto, A.; Fukuda, T.; Okubo, M., Iodine transfer dispersion polymerization (dispersion ITP) with CHI3 and reversible chain transfer catalyzed dispersion polymerization (dispersion RTCP) with GeI4 of styrene in supercritical carbon dioxide. *Polymer* **2012,** *53* (6), 1212-1218.
44. Hasell, T.; Thurecht, K. J.; Jones, R. D. W.; Brown, P. D.; Howdle, S. M., Novel one pot synthesis of silver nanoparticle-polymer composites by supercritical CO2 polymerisation in the presence of a RAFT agent. *Chem. Commun.* **2007,** (38), 3933-3935.
45. Zong, M. M.; Thurecht, K. J.; Howdle, S. M., Dispersion polymerisation in supercritical CO(2) using macro-RAFT agents. *Chem. Commun.* **2008,** (45), 5942-5944.

46. Lee, H.; Terry, E.; Zong, M.; Arrowsmith, N.; Perrier, S.; Thurecht, K. J.; Howdle, S. M., Successful dispersion polymerization in supercritical CO2 using polyvinylalkylate hydrocarbon surfactants synthesized and anchored via RAFT. *J. Am. Chem. Soc.* **2008,** *130* (37), 12242-+.
47. Birkin, N. A.; Wildig, O. J.; Howdle, S. M., Effects of poly(vinyl pivalate)-based stabiliser architecture on CO2-solubility and stabilising ability in dispersion polymerisation of N-vinyl pyrrolidone. *Polym. Chem.* **2013,** *4* (13), 3791-3799.
48. Huan, K.; Bes, L.; Haddleton, D. M.; Khoshdel, E., Synthesis and properties of polydimethylsiloxane-containing block copolymers via living radical polymerization. *J. Polym. Sci.; Part A: Polym. Chem.* **2001,** *39* (11), 1833-1842.
49. McHale, R.; Aldabbagh, F.; Zetterlund, P. B.; Okubo, M., Nitioxide-mediated radical precipitation polymerization of styrene in supercritical carbon dioxide. *Macromol. Chem. Phys.* **2007,** *208* (16), 1813-1822.
50. Aldabbagh, F.; Zetterlund, P. B.; Okubo, M., Improved control in nitroxide-mediated radical polymerization using supercritical carbon dioxide. *Macromolecules* **2008,** *41* (7), 2732-2734.
51. Aldabbagh, F.; Zetterlund, P. B.; Okubo, M., Nitroxide-mediated precipitation polymerization of styrene in supercritical carbon dioxide: Effects of monomer loading and nitroxide partitioning on control. *Eur. Polym. J.* **2008,** *44* (12), 4037-4046.
52. Magee, C.; Earla, A.; Petraitis, J.; Higa, C.; Braslau, R.; Zetterlund, P. B.; Aldabbagh, F., Synthesis of fluorinated alkoxyamines and alkoxyamine-initiated nitroxide-mediated precipitation polymerizations of styrene in supercritical carbon dioxide. *Polym. Chem.* **2014,** *5* (19), 5725-5733.
53. Israelachvili, J. N.; Mitchell, D. J.; Ninham, B. W., Theory of self-assembly of hydrocarbon amphiphiles into micelles and bilayers. *Journal of the Chemical Society - Faraday Transactions Ii* **1976,** *72*, 1525-1568.
54. Blanazs, A.; Armes, S. P.; Ryan, A. J., Self-Assembled Block Copolymer Aggregates: From Micelles to Vesicles and their Biological Applications. *Macromol. Rapid Commun.* **2009,** *30* (4-5), 267-277.
55. Mai, Y. Y.; Eisenberg, A., Self-assembly of block copolymers. *Chem. Soc. Rev.* **2012,** *41* (18), 5969-5985.
56. Bates, F. S., Polymer-polymer phase-behavior. *Science* **1991,** *251* (4996), 898-905.
57. Bates, F. S.; Fredrickson, G. H., Block copolymers - Designer soft materials. *Physics Today* **1999,** *52* (2), 32-38.
58. Luo, M.; Epps, T. H., Directed Block Copolymer Thin Film Self-Assembly: Emerging Trends in Nanopattern Fabrication. *Macromolecules* **2013,** *46* (19), 7567-7579.
59. Sun, Z. W.; Zhang, W. X.; Hong, S.; Chen, Z. B.; Liu, X. H.; Xiao, S. G.; Coughlin, E. B.; Russell, T. P., Using block copolymer architecture to achieve sub-10 nm periods. *Polymer* **2017,** *121*, 297-303.
60. Lodge, T. P.; Pudil, B.; Hanley, K. J., The full phase behavior for block copolymers in solvents of varying selectivity. *Macromolecules* **2002,** *35* (12), 4707-4717.

Graphical Abstract